Journal of Magnetic Resonance 193 (2008) 177–190

Contents lists available at ScienceDirect

Journal of Magnetic Resonance

journal homepage: www.elsevier.com/locate/jmr

Long-lived states in solution NMR: Theoretical examples in three- and four-spin systems

Aaron K. Grant *, Elena Vinogradov

Department of Radiology, Beth Israel Deaconess Medical Center, and Harvard Medical School, Ansin Building, Room 222, 330 Brookline Avenue, Boston, MA 02215, USA

ARTICLE INFO

Article history:
Received 3 March 2008
Revised 17 April 2008
Available online 24 April 2008

Keywords:
Long-lived states
Intramolecular dipolar relaxation
Singlet states

ABSTRACT

Long-lived spin states have been observed in a variety of systems. Although the dynamics underlying the long lifetimes of these states are well understood in the case of two-spin systems, the corresponding dynamics in systems containing more spins appear to be more complex. Recently it has been shown that a selection rule for transitions mediated by intramolecular dipolar relaxation may play a role in determining the lifetimes of long-lived states in systems containing arbitrary numbers of spins. Here we present a theory of long-lived states in systems containing three and four spins and demonstrate how it can be used to identify states that have little or no intramolecular dipolar relaxation.

1. Introduction

Recent work has demonstrated the existence of nuclear spin states with relaxation times significantly longer than the conventional spin–lattice relaxation time [1,2]. These states may have a variety of applications in NMR and biomedical imaging, including the study of 'slow' processes such as diffusion [3]. In the context of biomedical imaging, long-lived spin states may dramatically enhance the usefulness of hyperpolarized liquid contrast media [4,5]. These media, which can be imaged with a sensitivity many orders of magnitude greater than is possible using conventional techniques, are currently being investigated as tools for angiography [4,5], perfusion imaging [6,7], and metabolic studies aimed at cancer diagnosis [8–10]. However, the comparatively short spin–lattice relaxation times of the available agents limit their applications to the study of rapid processes that take place over timescales on the order of a few minutes. By combining hyperpolarization with long-lived states, it may be possible to prepare media that can be imaged with high sensitivity over extended periods of time.

Long-lived states have been observed in a variety of spin systems. In a generic two-spin system, the antisymmetric singlet state $|\alpha\beta\rangle - |\beta\alpha\rangle$ has been shown to persist up to 37 times longer than the T_1 relaxation times of constituent spins [3]. This lifetime prolongation is only observed when the effects of the chemical shift Hamiltonian are suppressed, either by placing the system in a weak magnetic field [1] or by applying suitable continuous radiofrequency (RF) irradiation at high field [2]. Several works have studied the effects of high magnetic fields on long-lived states and proposed RF irradiation schemes for lifetime prolongation at high field [2,11–14]. In some cases it is challenging to fully mitigate the effects of the chemical shift Hamiltonian using these methods. Consequently, in certain cases it may happen that lifetime prolongation is most readily achieved at low field. Long-lived states have also been observed in systems containing more than two spins, and have been prepared using both RF pulses [15] and parahydrogen-induced polarization [16,17].

In systems containing two spins, the singlet state is long-lived because it is immune to relaxation mediated by intramolecular dipolar interactions [14]. This immunity is a consequence of the fact that the singlet state, which is antisymmetric under exchange of the spins, cannot be converted into a symmetric triplet state by intramolecular dipolar interactions. In multi-spin systems, such symmetry arguments only apply in very specialized cases. The variety of long-lived states that have been observed experimentally suggests that other mechanisms may be at work. Various mechanisms that can give rise to long-lived states in multi-spins systems have been suggested, including *J*-stabilization [18] and quantum mechanical selection rules [19].

Here we discuss the implications of quantum mechanical selection rules for intramolecular dipolar relaxation in general spin systems at low field [19]. First, we show that these selection rules predict the existence of three- and four-spin states that are completely immune to intramolecular dipolar relaxation in the extreme narrowing limit. The extreme narrowing limit [20] is a good approximation for many systems of interest, particularly at low field, and provides some simplification of the analysis. Deviations from the extreme narrowing limit for small molecules in solution NMR are not expected to qualitatively modify our

* Corresponding author. Fax: +1 617 667 7917.
E-mail address: akgrant@bidmc.harvard.edu (A.K. Grant).

1090-7807/$ - see front matter © 2008 Published by Elsevier Inc.
doi:10.1016/j.jmr.2008.04.030

conclusions, but are worthy of further study. The immunity of these long-lived states from intramolecular dipolar relaxation is the consequence of a 'bottleneck' in the relaxation process that is imposed by the selection rules and that prevents populations in certain states from coming into equilibrium with others. Such bottlenecks do not occur in arbitrary systems, but only in certain systems where the spins are located at specific spatial locations within the tumbling molecule. Hence, another consequence of these selection rules is that it is possible to derive a purely geometrical criterion that determines whether a particular spin system can have states with vanishing dipolar relaxation, independent of any consideration of the *J*-couplings. For those systems that do not possess states that are totally immune to dipolar relaxation, the selection rules can be used to determine optimal combinations of scalar couplings that minimize the dipolar decay rate. Finally, we highlight certain differences between systems with more than four spins and those with four or fewer spins. Although systems with more than four strongly coupled spins may have long-lived states, these states require a relatively complex cancellation among various decay rates.

It is possible that many mechanisms of lifetime prolongation in addition to those described here are relevant to the dynamics of long-lived states. In particular, proof that a system does not have a selection rule relaxation bottleneck does not constitute proof that the system has no long-lived states of any kind. To avoid potential confusion stemming from this issue, we will refer to states that are long-lived because of selection rules and relaxation bottlenecks as 'dipolar selection rule' (DSR) long-lived states, or simply as 'DSR states.' We will refer to states whose dipolar relaxation rates vanish exactly in the extreme narrowing limit as 'exact' DSR states. In addition to states of this kind, we find that certain multi-spin systems possess long-lived population imbalances whose lifetimes are prolonged because of a discrete exchange symmetry similar to that seen in systems containing two spins [14]. Furthermore, certain DSR states decompose into pairwise combinations of singlets that are long-lived for many of the same reasons as a singlet state of two spins. Apart from such 'singlet-like' states, however, there are many examples of DSR states that do not contain singlet combinations and that have no particular exchange symmetries.

In the following sections we present a brief overview of selection rules in intramolecular dipolar relaxation, and give a detailed account of the low-field energy eigenstates of the three- and four-spin systems. We find that in the three-spin system, only systems where the three spins are collinear have states whose dipolar relaxation rates vanish exactly. By contrast, in the four-spin system, such states occur in linear, planar, and fully three-dimensional systems. Perhaps surprisingly, we find that two highly symmetric cases, one where three spins are placed at the vertices of an equilateral triangle, and another where four spins are placed at the vertices of a tetrahedron, do not possess exact DSR states.

We have not yet conducted a systematic survey of molecular structures to ascertain which, if any, of the combinations of geometries and scalar couplings described here can be realized in practice. Rather, our intention is to describe a method for identifying geometries and couplings that give rise to long-lived states, and to demonstrate that such states can, in principle, exist in a variety of systems. The expressions provided here can be used to select promising candidates for further studies of long-lived states. We note that, in many cases, both positive and negative scalar couplings with widely varying magnitudes are necessary to attain complete immunity to dipolar relaxation.

In addition to the work already cited, certain earlier papers have identified geometries of three-spin systems that are immune to intramolecular dipolar interactions and hence can possess long-lived DSR states as described here. In [21,22] it was noted that linear three-spin systems with suitable couplings possess states immune to intramolecular dipolar relaxation. Similar states have been identified in triangular three-spin systems that are free to rotate about their axis of symmetry but that are fixed with respect to other axes [23].

2. The Hamiltonian and the energy eigenstates

Consider a spin system consisting of N coupled spins where the chemical shift Hamiltonian is negligible in comparison to the scalar couplings. The effects of the chemical shift Hamiltonian can be eliminated by placing the system in a sufficiently weak magnetic field [1] or by subjecting the system to suitable RF irradiation at high field [2]. In the following, we will refer to all such conditions as 'low field' conditions. In the low field limit, the Hamiltonian for such a spin system consists of scalar couplings only:

$$H_0 = \sum_{k,l=1;k<l}^{N} 2\pi J_{kl} \vec{I}_k \cdot \vec{I}_l. \tag{1}$$

Because the Hamiltonian is invariant under spatial rotations, the eigenstates of this Hamiltonian are also eigenstates of the total spin angular momentum $\vec{I}^2 = \left(\sum_k \vec{I}_k\right)^2$ and its z-component $I_z = \sum_k \vec{I}_{k,z}$. We may therefore denote the energy eigenstates by $|jm, E\rangle$, where j is the total spin angular momentum, m is the magnetic quantum number $m = -j \ldots + j$, and E is the energy of the state. As examples, the three-spin system possesses a single $j = 3/2$ multiplet and two distinct $j = 1/2$ doublets (for a total of 8 states), while the four-spin system possesses a single $j = 2$ multiplet, three $j = 1$ triplets, and two $j = 0$ singlets (for a total of 16 states). The eigenstates are schematically depicted in Fig. 1. In the following discussion we will assume that there are no accidental degeneracies between the states with the same total spin j.

The foregoing discussion can be made explicit by evaluating the matrix elements of the Hamiltonian of Eq. (1) in a basis of total

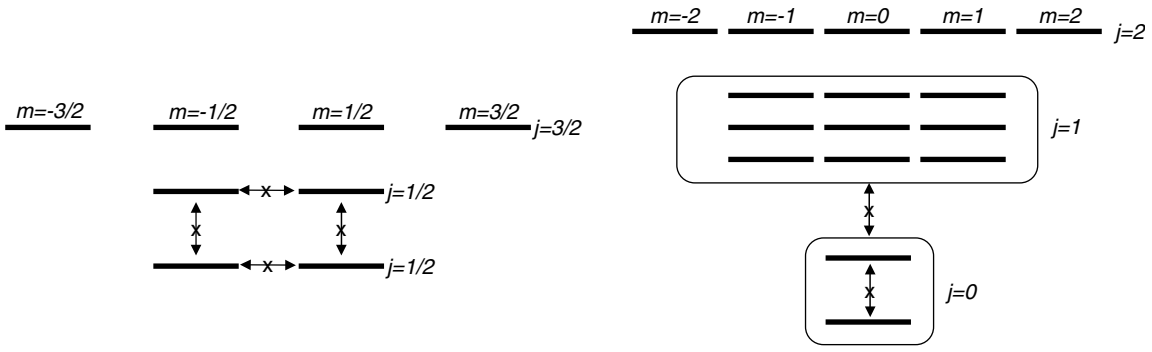

Fig. 1. Left: Energy levels and forbidden transitions (indicated by crossed arrows) in the three-spin system. Right: Energy levels and forbidden transitions in the four-spin system. On the right, the single crossed arrow between the $j = 0$ and $j = 1$ multiplets indicates that *all* $j = 0$-to-$j = 1$ transitions are forbidden.

spin eigenstates. The choice of basis is somewhat arbitrary, and so we adopt the following procedure for establishing a basis. For each value of j, we select an orthonormal basis of states having the maximal magnetic quantum number m. We then determine the states with lower values of m by applying the lowering operator $I_- = \sum_k I_{k,-}$, where $I_{k,-} = (I_{k,x} - iI_{k,y})/\sqrt{2}$, as many times as necessary to complete the multiplet. The resulting states are then normalized to unity without modification of their complex phase.

2.1. The three-spin system

In the three spin system the $j = 3/2$ states are given by

$$|3/2, m\rangle \propto \{|\alpha\alpha\alpha\rangle, I_-|\alpha\alpha\alpha\rangle, I_-^2|\alpha\alpha\alpha\rangle, I_-^3|\alpha\alpha\alpha\rangle\} \tag{2}$$

for $m = 3/2, 1/2, -1/2, -3/2$, respectively. For brevity we have omitted the normalization factors of the lower m states. In addition, we must specify a basis for two distinct $j = 1/2$ subspaces. We distinguish these doublets using labels 'A' and 'B'. For the A doublet, we choose a pair of states with spins 2 and 3 in a singlet state. Explicitly, the $m = 1/2$ state is given by $|1/2, 1/2\rangle_A = (|\alpha\beta\rangle - |\alpha\beta\alpha\rangle)/\sqrt{2}$, and the complete doublet is given by

$$|1/2, m\rangle_A \propto \{|1/2, 1/2\rangle_A, I_-|1/2, 1/2\rangle_A\}. \tag{3}$$

The B doublet is then uniquely specified, up to a phase, by the requirement that it be orthogonal to the A doublet of Eq. (3). We may choose $|1/2, 1/2\rangle_B = (2|\beta\alpha\alpha\rangle - |\alpha\alpha\beta\rangle - |\alpha\beta\alpha\rangle)/\sqrt{6}$, and

$$|1/2, m\rangle_B \propto \{|1/2, 1/2\rangle_B, I_-|1/2, 1/2\rangle_B\}. \tag{4}$$

The states in Eqs. (3) and (4) are eigenstates of the total spin, but are *not* (in general) eigenstates of the Hamiltonian in Eq. (1).

The rotational invariance of the Hamiltonian in Eq. (1) implies that it is block diagonal in the quantum numbers j and m. Ordering the basis elements from Eqs. (2)–(4) as $\{|3/2, 3/2\rangle, \ldots, |3/2, -3/2\rangle, |1/2, 1/2\rangle_A, |1/2, 1/2\rangle_B, |1/2, -1/2\rangle_A, |1/2, -1/2\rangle_B\}$, the matrix form of H, in block notation, is

$$H = \begin{bmatrix} H_{j=3/2} & 0 & 0 \\ 0 & H_{j=1/2,m=1/2} & 0 \\ 0 & 0 & H_{j=1/2,m=-1/2} \end{bmatrix} \tag{5}$$

where $H_{j=3/2}$ is a diagonal matrix with all diagonal entries equal to $\pi(J_{12} + J_{13} + J_{23})/2 \equiv \pi\bar{J}/2$, and the $j = 1/2$ blocks are given by

$$H_{j=1/2,m=1/2} = H_{j=1/2,m=-1/2} = \frac{\pi}{2}\begin{bmatrix} -3J_{23} & \sqrt{3}(J_{13} - J_{12}) \\ \sqrt{3}(J_{13} - J_{12}) & J_{23} - 2J_{13} - 2J_{12} \end{bmatrix}. \tag{6}$$

Because the $j = 3/2$ block of the Hamiltonian is already diagonal, the diagonalization of the Hamiltonian reduces to the problem of diagonalizing the two-by-two matrix in Eq. (6). The resulting eigenstates can be expressed in terms of the states A and B given in Eqs. (3) and (4) in terms of a single mixing angle, which we denote by ψ_3 for the three-spin system. The energy eigenvalues in the $j = 1/2$ subspace are determined by a two-by-two diagonalization, and are given by

$$\begin{aligned} E_\pm &= \frac{\pi}{2}\left(-\bar{J} \pm 2\sqrt{J_{12}^2 + J_{13}^2 + J_{23}^2 - J_{12}J_{23} - J_{13}J_{23} - J_{12}J_{13}}\right) \\ &\equiv \frac{\pi}{2}(-\bar{J} \pm \Delta) \end{aligned} \tag{7}$$

(recall that $\bar{J} = J_{12} + J_{13} + J_{23}$), and the corresponding eigenstates are given by

$$\begin{aligned} |1/2, m, E_+\rangle &= \cos\psi_3|1/2, m\rangle_A + \sin\psi_3|1/2, m\rangle_B, \\ |1/2, m, E_-\rangle &= -\sin\psi_3|1/2, m\rangle_A + \cos\psi_3|1/2, m\rangle_B, \end{aligned} \tag{8}$$

where the mixing angle ψ_3 is given in terms of the scalar couplings J_{kl} by

$$\psi_3(J_{kl}) = \tan^{-1}\frac{-J_{12} - J_{13} + 2J_{23} + \Delta}{\sqrt{3}(-J_{12} + J_{13})}. \tag{9}$$

We choose a branch of the inverse tangent such that the range of ψ_3 is $-\pi/2 < \psi_3 \leqslant \pi/2$. From Eqs. (6)–(9), we see that the energy eigenbasis is specified by a single dimensionless function of the scalar couplings, namely the mixing angle ψ_3.

For future reference, we note that the states $|1/2, m, E_+\rangle$ contain a singlet combination of spins at the following values of ψ_3: For $\psi_3 = 0$, $|1/2, m, E_+\rangle$ contains a singlet of spins 2 and 3, while for $\psi_3 = \pi/3$, $|1/2, m, E_+\rangle$ contains a singlet of spins 1 and 2. In addition, for $\psi_3 = -\pi/3$, $|1/2, m, E_+\rangle$ corresponds to a singlet of spins 1 and 3. The states $|1/2, m, E_-\rangle$ contain a singlet combination of spins at values of ψ_3 shifted by $-\pi/2$. This is an exhaustive list of all singlet combinations because it includes all pairwise combinations of the spins.

2.2. The four-spin system

The analysis of the four-spin system proceeds as in Eqs. (2)–(9). As in the three-spin system, the states of highest spin, in this case $j = 2$, are readily found:

$$|2, m\rangle \propto \{|\alpha\alpha\alpha\alpha\rangle, I_-|\alpha\alpha\alpha\alpha\rangle, I_-^2|\alpha\alpha\alpha\alpha\rangle, I_-^3|\alpha\alpha\alpha\alpha\rangle, I_-^4|\alpha\alpha\alpha\alpha\rangle\}. \tag{10}$$

The four-spin system possesses three spin-one triplets. We label these states as $|1, m\rangle_A$, $|1, m\rangle_B$, and $|1, m\rangle_C$. An orthogonal basis of $j = 1$, $m = 1$ states is given by

$$\begin{aligned} |1, 1\rangle_A &= \frac{1}{2}(|\alpha\alpha\beta\alpha\rangle - |\alpha\alpha\beta\alpha\rangle - |\alpha\beta\alpha\alpha\rangle + |\beta\alpha\alpha\alpha\rangle) \\ |1, 1\rangle_B &= \frac{1}{2}(|\alpha\alpha\beta\alpha\rangle - |\alpha\alpha\beta\alpha\rangle + |\alpha\beta\alpha\alpha\rangle - |\beta\alpha\alpha\alpha\rangle) \\ |1, 1\rangle_C &= \frac{1}{2}(|\alpha\alpha\beta\alpha\rangle + |\alpha\alpha\beta\alpha\rangle - |\alpha\beta\alpha\alpha\rangle - |\beta\alpha\alpha\alpha\rangle). \end{aligned} \tag{11}$$

States with lower m values are obtained by applying the lowering operator I_-. The four-spin basis is completed by two $j = 0$ states, which we label as $|0, 0\rangle_A$, and $|0, 0\rangle_B$. We choose the state $|0, 0\rangle_A$ to be that state in which spins one and two are in a singlet state, while the third and fourth form a second singlet:

$$|0, 0\rangle_A = \frac{1}{2}(|\alpha\beta\alpha\beta\rangle - |\alpha\beta\beta\alpha\rangle - |\beta\alpha\alpha\beta\rangle + |\beta\alpha\beta\alpha\rangle) \tag{12}$$

The B state is determined, up to a phase, by the requirement that it is orthogonal to the state in Eq. (12) and that it is an eigenstate of the total spin with eigenvalue 0. We choose

$$|0, 0\rangle_B = \frac{1}{2\sqrt{3}}(2|\alpha\alpha\beta\beta\rangle + 2|\beta\beta\alpha\alpha\rangle - |\alpha\beta\beta\alpha\rangle - |\beta\alpha\alpha\beta\rangle - |\alpha\beta\alpha\beta\rangle - |\beta\alpha\beta\alpha\rangle). \tag{13}$$

As before, the Hamiltonian is block-diagonal, and in block notation takes the form

$$H = \begin{bmatrix} H_{j=2} & 0 & 0 & 0 & 0 \\ 0 & H_{j=1,m=1} & 0 & 0 & 0 \\ 0 & 0 & H_{j=1,m=0} & 0 & 0 \\ 0 & 0 & 0 & H_{j=1,m=-1} & 0 \\ 0 & 0 & 0 & 0 & H_{j=0} \end{bmatrix}. \tag{14}$$

The $j = 2$ block is a diagonal matrix with all diagonal entries equal to $\pi(\sum_{k<l} J_{kl})/2$. The $j = 1$ blocks will not be needed for the analysis of relaxation bottlenecks and so are omitted for brevity. The $j = 0$ block is given by the two-by-two matrix

$$H_{j=0} = \frac{\pi}{2}\begin{bmatrix} -3(J_{12} + J_{34}) & -\sqrt{3}(J_{13} - J_{14} - J_{23} + J_{24}) \\ -\sqrt{3}(J_{13} - J_{14} - J_{23} + J_{24}) & J_{12} - 2J_{13} - 2J_{14} - 2J_{23} - 2J_{24} + J_{34} \end{bmatrix}. \tag{15}$$

The $j = 0$ energy eigenbasis is specified by a single mixing angle, which we denote by ψ_4 to emphasize that it plays an analogous role to the corresponding mixing angle in the three-spin case. Explicitly, we have

$$|0,0,E_+\rangle = \cos\psi_4|0,0\rangle_A + \sin\psi_4|0,0\rangle_B,$$
$$|0,0,E_-\rangle = -\sin\psi_4|0,0\rangle_A + \cos\psi_4|0,0\rangle_B. \tag{16}$$

The expressions for ψ_4 and the energies $E_\pm$ are lengthy and have been given in Appendix A.1. As in the three-spin case, we have $-\pi/2 < \psi_4 \leqslant \pi/2$. Furthermore, as in the three-spin case, the low-field energy eigenstates in the $j = 0$ and $j = 2$ manifolds are specified completely in terms of a single dimensionless function of the scalar couplings, namely the mixing angle ψ_4.

Although we forego a detailed discussion of the $j = 1$ energy eigenbasis, we note that the eigenstates can be specified in terms of the states in Eq. (11) and three mixing angles. Each block of the $j = 1$ Hamiltonian is a three-by-three matrix that can be diagonalized by a three-by-three orthogonal transformation that is conveniently specified in terms of three Euler angles (α, β, γ). These angles are independent of m by rotational symmetry. For the $j = 1, m = 1$ states, we have

$$\begin{pmatrix} |1,1,E_1\rangle \\ |1,1,E_2\rangle \\ |1,1,E_3\rangle \end{pmatrix} = \begin{pmatrix} \cos\gamma & \sin\gamma & 0 \\ -\sin\gamma & \cos\gamma & 0 \\ 0 & 0 & 1 \end{pmatrix} \begin{pmatrix} 1 & 0 & 0 \\ 0 & \cos\beta & \sin\beta \\ 0 & -\sin\beta & \cos\beta \end{pmatrix} \times \begin{pmatrix} \cos\alpha & \sin\alpha & 0 \\ -\sin\alpha & \cos\alpha & 0 \\ 0 & 0 & 1 \end{pmatrix} \begin{pmatrix} |1,1\rangle_A \\ |1,1\rangle_B \\ |1,1\rangle_C \end{pmatrix}, \tag{17}$$

and similarly for the $m = 0, -1$ states.

For future reference, we note that the state $|0,0,E_+\rangle$ reduces to a combination of pairwise singlet states at the following values of ψ_4: for $\psi_4 = 0, |0,0,E_+\rangle$ corresponds to a singlet of spins 1 and 2 together with a singlet of spins 3 and 4. For $\psi_4 = \pi/3, |0,0,E_+\rangle$ corresponds to a singlet of spins 1 and 3 together with a singlet of spins 2 and 4, while for $\psi_4 = -\pi/3, |0,0,E_+\rangle$ corresponds to a singlet of spins 1 and 4 together with a singlet of spins 2 and 3. The state $|0,0,E_-\rangle$ contains a singlet combination of spins at values of ψ_4 that are shifted by $\psi_4 \to \psi_4 - \pi/2$. Since this list includes all pairwise combinations of the spins, it is an exhaustive list of all singlet combinations.

3. Transition rates

Using a given basis of energy eigenstates, we can compute the transition rates between these states that result from intramolecular dipolar interactions. The intramolecular dipolar Hamiltonian is given by

$$H_{DD} = -\sqrt{\frac{8\pi}{15}}\sum_{k=1}^{N-1}\sum_{l=k+1}^{N}\sum_{M=-2}^{2} b_{kl}Y_{2,-M}(\hat{r}_{kl})T^{kl}_{2,M} \tag{18}$$

where $b_{kl} = 3\mu_0\gamma^2\hbar/4\pi r_{kl}^3$, $\vec{r}_{kl}$ is the (time-dependent) vector connecting spins k and l, and the spin operators $T^{kl}_{2,M}$ are given by

$$T^{kl}_{20} = \frac{1}{\sqrt{6}}\{2I^k_zI^l_z - (I^k_+I^l_- + I^k_-I^l_+)\},$$
$$T^{kl}_{2\pm1} = \pm\frac{1}{\sqrt{2}}\{I^k_zI^l_\pm + I^k_\pm I^l_z\}, \quad T^{kl}_{2\pm2} = I^k_\pm I^l_\pm. \tag{19}$$

The expression for the transition rate between a pair of states $|a\rangle$ and $|b\rangle$ is given by [20]

$$W_{a\to b} = \int_{-\infty}^{+\infty}\overline{\langle a|H_{DD}(t)|b\rangle\langle b|H_{DD}(t+\tau)|a\rangle}e^{-i(E_a-E_b)\tau} = \frac{8\pi}{15}\sum_{ij,kl,M,M'} b_{ij}b_{kl}\langle a|T^{ij}_M|b\rangle\langle b|T^{kl}_{M'}|a\rangle \times \int_{-\infty}^{+\infty}\overline{Y_{2M}(\hat{r}_{ij}(t))Y_{2M'}(\hat{r}_{kl}(t+\tau))}e^{-i(E_a-E_b)\tau} \tag{20}$$

In the extreme narrowing limit the correlation function is given by [23]

$$\int_{-\infty}^{+\infty}\overline{Y_{2M}(\hat{r}_{ij}(t))Y_{2M'}(\hat{r}_{kl}(t+\tau))}e^{-i(E_a-E_b)\tau} = (-1)^M\frac{\tau_c}{4\pi}\delta_{M,-M'}P_2(\cos\theta_{ij,kl}), \tag{21}$$

where $\theta_{ij,kl}$ is the angle, in the frame of the molecule, between $\hat{r}_{ij}$ and $\hat{r}_{kl}$, and τ_c is the correlation time for the molecular tumbling. P_2 is the second order Legendre polynomial. From this, we obtain

$$W_{a\to b} = \frac{2\tau_c}{15}\sum_{ij,kl,M}(-1)^M b_{ij}b_{kl}\langle a|T^{ij}_M|b\rangle\langle b|T^{kl}_{-M}|a\rangle P_2(\cos\theta_{ij,kl}). \tag{22}$$

For purposes of subsequent calculations, we have implemented the sum in Eq. (20) using Mathematica (Wolfram Research, Champaign, Illinois).

The matrix element $\langle jm,E|H_{DD}(t)|j'm',E'\rangle$ is subject to a selection rule [19], and vanishes unless j is in the range $|j'-2|, |j'-2|+1, \ldots, j'+2$:

$$\langle jm,E|H_{DD}(t)|j'm',E'\rangle = 0 \quad \text{if } j \neq |j'-2|,\ldots,j'+2 \tag{23}$$

Consequently, in the three-spin system, the intramolecular dipolar transition rates between any pair of $j = 1/2$ states vanish identically; only transitions between $j = 1/2$ and $j = 3/2$ are allowed. Similarly, in the four-spin system, transitions between the $j = 0$ states are forbidden, as are transitions between the $j = 0$ and $j = 1$ states. Of course, this is not to say that a population in the three-spin system cannot migrate from one $j = 1/2$ state to the other. However, the selection rule in Eq. (23) does mean that such a migration can only be achieved by a two-stage process where the system passes first through the $j = 3/2$ state and then subsequently back to the $j = 1/2$ states. Similarly, in the four-spin system, populations in the $j = 0$ states can only equilibrate via intermediate transitions to the $j = 2$ states. The pattern of allowed and forbidden transitions illustrated in Fig. 1.

The above considerations show that in the three- and four-spin systems the only allowed transitions from the lowest spin states are those to highest spin states (namely from $j = 1/2$ to $j = 3/2$ in the three-spin case, and from $j = 0$ to $j = 2$ in the four-spin case). Because the highest-spin energy eigenstates are independent of the scalar couplings, and because the lowest-spin energy eigenstates depend on the scalar couplings only through a single mixing angle (ψ_3 or ψ_4), the transition rates to and from the lowest spin states likewise depend on the scalar couplings only through a single mixing angle. Hence, the transition rates to and from the lowest-spin energy eigenstates of the three- and four-spin systems have a simple dependence on the scalar couplings.

The upshot of this discussion is that the decay rates of the lowest spin states in the three- and four-spin systems are functions of (i) the geometry of the molecule under consideration and (ii) a single mixing angle that depends implicitly upon the scalar couplings of the system. Mathematically, the rate matrix W in Eq. (22) has the property that, for any given lowest-spin state,

$$\sum_X W_{|\text{Lowest spin}\rangle\to|X\rangle} = F(\psi_N, \{\vec{r}_1, \vec{r}_2, \ldots\}), \tag{24}$$

where the sum extends over all accessible final states X, $\vec{r}_k$ are the body-frame coordinates of the spins, and N =3 or 4.

The subsequent analysis is simplified by two final observations regarding the rate matrix in Eq. (22). First, as a consequence of the form of the dipolar Hamiltonian, the rate matrices for two molecules that have the same shape but different overall sizes will differ only by a factor equal to the sixth power of the ratio of their sizes. Second, the rate in Eq. (24) involves two factors of the lowest-spin energy eigenstates (see Eq. (20)). Substitution of the eigenstates given in Eqs. (2) and (8) for three-spin case and Eqs. (10) and (16) for the four-spin case results in expressions that are quadratic in the sine and cosine of the mixing angle. Using the double-angle formula and noting that the E_+ and E_- energy eigenstates in Eqs. (8) and (16) differ only by the substitution $\psi_N \to \psi_N + \pi/2$, Eq. (24) can be written in the form

$$\sum_X W_{|\text{Lowest spin},E_\pm\rangle \to |X\rangle} = \frac{3\mu_0^2\gamma^4\hbar^2\tau_c}{40\pi^2 r_{12}^6}[A(\vec{\rho}_1,\vec{\rho}_2,\ldots) + B(\vec{\rho}_1,\vec{\rho}_2,\ldots)\cos(2\psi_N+\delta_\pm) + C(\vec{\rho}_1,\vec{\rho}_2,\ldots)\sin(2\psi_N+\delta_\pm)] \tag{25}$$

where $\vec{\rho}_k = \vec{r}_k/r_{12}$ is the (dimensionless) radius vector of the k^{th} spin, scaled by the distance between spins 1 and 2. The functions A, B, and C are dimensionless functions of the system's geometry. The phase $\delta_\pm$ is equal to 0 for the E_+ states and π for the E_- states. Because the mixing angles have the range $-\pi/2 < \psi_N \leqslant \pi/2$, the arguments of the sine and cosine in Eq. (25) cover the entire range from 0 to 2π for both the E_+ states and the E_- states. Hence, if the decay rate of the E_+ state vanishes for a given value of ψ_N, there will always be a second, corresponding configuration where ψ_N is shifted by $\pi/2$ and the E_- state is long-lived. In the following sections, we will work in terms of the E_+ state, with the understanding that all of the results can be translated in a one-to-one way for the E_- state as well.

Eq. (25) provides the starting point for a systematic search for systems with relaxation bottlenecks and long-lived states. Indeed, differentiating Eq. (25) with respect to ψ_N shows that the extrema are located at values of ψ_N satisfying $\tan(2\psi_N+\delta_\pm) = C/B$. Inverting this equation and choosing the appropriate branch of the inverse tangent gives the absolute minimum, which in turn provides a lower bound on the transition rate:

$$\sum\nolimits_X W_{|\text{Lowest spin},E_\pm\rangle\to|X\rangle} \geqslant L \equiv \frac{3\mu_0^2\gamma^4\hbar^2\tau_c}{40\pi^2 r_{12}^6}[A(\vec{\rho}_1,\vec{\rho}_2,\ldots) - \sqrt{B(\vec{\rho}_1,\vec{\rho}_2,\ldots)^2 + C(\vec{\rho}_1,\vec{\rho}_2,\ldots)^2}]. \tag{26}$$

For three- and four-spins systems, the quantity L provides a purely geometrical lower bound on the decay rates of the lowest spin states that is independent of the particular values of the scalar couplings. Qualitatively speaking, geometrical configurations of spins that have large values of L are unlikely to have long-lived DSR states, regardless of their scalar couplings. On the other hand, configurations that have small (or vanishing) values of L will possess long-lived DSR states provided that the scalar couplings lead to mixing angles that satisfy, at least approximately, the criterion $\tan(2\psi_N+\delta_\pm) = C/B$. Consequently we see that a necessary (but not sufficient) condition for the existence of a state whose dipolar relaxation rate exactly vanishes (that is, an 'exact' DSR state) is that the quantity in brackets in Eq. (26) vanishes. Defining

$$D(\vec{\rho}_1,\vec{\rho}_2,\cdots) = A(\vec{\rho}_1,\vec{\rho}_2,\cdots) - \sqrt{B(\vec{\rho}_1,\vec{\rho}_2,\cdots)^2 + C(\vec{\rho}_1,\vec{\rho}_2,\cdots)^2}, \tag{27}$$

we conclude that if a system possesses an exact DSR state, then D must vanish. The converse is not true: if the scalar couplings do not obey $\tan(2\psi_N+\delta_\pm) = C/B$, it is possible for a system to have D=0 without also having an exact DSR state. Because the criterion in Eq. (27) does not involve the scalar couplings, we can use this condition to determine, from purely geometrical considerations, whether it is possible for a system to have a long-lived DSR state.

The quantity D in Eq. (27) enables us to determine geometrical configurations of spins that may potentially possess DSR states, but says nothing about the scalar couplings that are required in order to obtain such a state. In order to establish the existence of an exact DSR state in a physically realizable system, we must determine combinations of scalar couplings that yield the mixing angle for which the right-hand side of Eq. (25) vanishes. In Appendix A.2 it is shown that for the three- and four-spin cases, this is always mathematically possible. In practice, we find that the families of scalar couplings required for exact DSR states often contain both positive and negative couplings.

A measure of the lifetime enhancement that can result from the mechanisms described above can be obtained by comparing the decay rates of states at high and low field. To do so, we must compute the rate matrix Eq. (22) for a suitable set of high-field energy eigenstates. In general, these high-field eigenstates will depend upon a large number of parameters, including the scalar couplings and chemical shifts of the system. However, a reasonable estimate of the eigenstates can be obtained by noting that in the high-field limit, the scalar couplings in many (but by no means all) systems are small compared to the chemical shifts. In this limit, the Zeeman interaction dominates and the energy eigenstates are given, approximately, by the product spin states $|\alpha\alpha\alpha\rangle, |\alpha\alpha\beta\rangle$, etc. Given the rate matrices W^{high} and W^{low} at high and low field, the time dependence of the vector ρ of populations is determined by the rate equations [20]

$$\frac{d\rho_a}{dt} = \sum_b \left(W_{ab} - \delta_{ab}\sum_c W_{ac}\right)(\rho_b - \rho_b^{\text{Equilibrium}}). \tag{28}$$

The solution to Eq. (28) is a linear combination of exponentially decaying terms that tends towards the equilibrium solution as $t \to \infty$. The longest-lived population imbalance is dictated by the smallest non-trivial eigenvalue of the matrix in parentheses in Eq. (28) (the matrix always possesses a trivial zero eigenvalue corresponding to the equilibrium state). We may quantify the ratio of high-field and low-field lifetimes in terms of an 'enhancement factor' E given by

$$E = \frac{\text{Smallest non-trivial eigenvalue of}(W_{ab}^{\text{High}} - \delta_{ab}\sum_c W_{ac}^{\text{High}})}{\text{Smallest non-trivial eigenvalue of}(W_{ab}^{\text{Low}} - \delta_{ab}\sum_c W_{ac}^{\text{Low}})}. \tag{29}$$

4. Results and discussion

4.1. Three-spin systems

We consider a three-spin system with geometry as illustrated in Fig. 2. This geometry is general enough to encompass any configuration of three spins. Without loss of generality we label the spins such that spins 1 and 2 are closer than spins 1 and 3, and we scale the radii (as in Eq. (25)) such that the distance between spins 1 and 2 is equal to unity. The full molecular geometry is then specified by the angle θ between $\vec{r}_{12}$ and $\vec{r}_{13}$ and the dimensionless ratio $\lambda = r_{13}/r_{12}$. By our labeling convention λ is always greater than or equal to 1. In the basis

$$\{|3/2,3/2\rangle,\ldots,|3/2,-3/2\rangle,|1/2,1/2,E_-\rangle,|1/2,-1/2,E_-\rangle, |1/2,1/2,E_+\rangle,|1/2,-1/2,E_+\rangle\}, \tag{30}$$

the rate matrix takes the form [19]

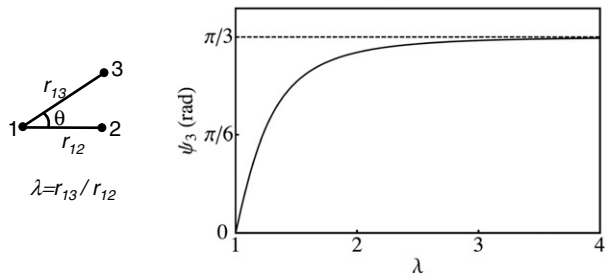

Fig. 2. Left: Geometry of a generic three-spin system. Right: Mixing angle that yields a state with vanishing dipolar decay rate (i.e., an exact DSR state) as a function of λ in the linear three-spin system.

$$W=\frac{3\mu_0^2\gamma^4\hbar^2\tau_c}{40\pi^2 r_{12}^6}\left(\begin{array}{cccc|cc|cc}
w_{3/2} & 2w_{3/2} & 2w_{3/2} & 0 & w_- & 4w_- & w_+ & 4w_+\\
2w_{3/2} & w_{3/2} & 0 & 2w_{3/2} & 2w_- & 3w_- & 2w_+ & 3w_+\\
2w_{3/2} & 0 & w_{3/2} & 2w_{3/2} & 3w_- & 2w_- & 3w_+ & 2w_+\\
0 & 2w_{3/2} & 2w_{3/2} & w_{3/2} & 4w_- & w_- & 4w_+ & w_+\\
\hline
w_- & 2w_- & 3w_- & 4w_- & 0 & 0 & 0 & 0\\
4w_- & 3w_- & 2w_- & w_- & 0 & 0 & 0 & 0\\
\hline
w_+ & 2w_+ & 3w_+ & 4w_+ & 0 & 0 & 0 & 0\\
4w_+ & 3w_+ & 2w_+ & w_+ & 0 & 0 & 0 & 0
\end{array}\right) \tag{31}$$

where $w_{3/2}$ depends on the geometrical parameters λ and θ, while w_- and w_+ depend also upon the mixing angle ψ_3. Because of the similarity between the states $|1/2,1/2,E_+\rangle$ and $|1/2,1/2,E_-\rangle$, the function w_- differs from w_+ only through the substitution $\psi_3 \to \psi_3+\pi/2$. The expression in Eq. (25) for the lowest-spin state $|1/2,1/2,E_+\rangle$ is given by

$$\begin{aligned}\sum\nolimits_{\mathrm{X}} w_{|1/2,1/2,E_+\rangle\to|\mathrm{X}\rangle} &= \frac{3\mu_0^2\gamma^4\hbar^2\tau_c}{40\pi^2 r_{12}^6}[10w_+]\\ &\equiv \frac{3\mu_0^2\gamma^4\hbar^2\tau_c}{40\pi^2 r_{12}^6}[A(\lambda,\theta)+B(\lambda,\theta)\cos 2\psi_3\\ &\quad + C(\lambda,\theta)\sin 2\psi_3].\end{aligned} \tag{32}$$

The complete expressions for A, B, and C are given in Appendix A.3.

We now turn to particular molecular geometries.

4.1.1. Linear systems

The simplest example of a linear symmetric system is given by $\lambda=1$ and $\theta=\pi$ (see Fig. 2). In this case,

$$\begin{aligned}&[A(\lambda,\theta)+B(\lambda,\theta)\cos 2\psi_3+C(\lambda,\theta)\sin 2\psi_3]_{\lambda=1,\theta=\pi}\\ &\quad=\frac{245}{1536}(1-\cos 2\psi_3)\end{aligned} \tag{33}$$

From this we immediately see that for $\psi_3=0$, the state $|1/2,1/2,E_+\rangle$ is immune to intramolecular dipolar relaxation and should therefore be long-lived (i.e., it is an exact DSR state). More explicitly, this means that the state in which the spins at the ends of the molecule (in this case, spins 2 and 3) are in a singlet state is long-lived. In terms of scalar couplings, this corresponds to the case $J_{12}=J_{13}$, with arbitrary J_{23}.

It is worth demonstrating explicitly how this long-lived state comes about. To this end, consider the transition from $|1/2,1/2,E_+\rangle$ to the spin-3/2 state $|3/2,3/2\rangle=|\alpha\alpha\alpha\rangle$. For $\psi_3=0$, we have

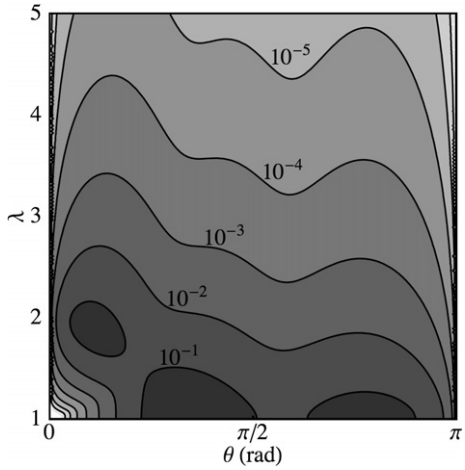

Fig. 3. Discriminant function D from Eq. (27) as a function of λ and θ in the three-spin system. The distance r_{12} has been scaled to 1. Smaller values of D correspond to longer lifetimes.

$$|1/2,1/2,E_+\rangle_{\psi_3=0}=|1/2,1/2\rangle_A=(|\alpha\alpha\beta\rangle-|\alpha\beta\alpha\rangle)/\sqrt{2}. \tag{34}$$

It is useful to decompose the intramolecular dipolar Hamiltonian into a sum of pairwise interactions: $H_{DD}\equiv H_{DD}^{12}+H_{DD}^{13}+H_{DD}^{23}$. At any given instant of time, the highly symmetric forms of the states $|1/2,1/2,E_+\rangle$ and $|3/2,3/2\rangle$ lead to the following simple relationships between the matrix elements of the different terms in H_{DD}:

$$\begin{aligned}&\langle 3/2,3/2|H_{DD}^{12}|1/2,1/2,E_+\rangle_{\psi_3=0}=-\langle 3/2,3/2|H_{DD}^{13}|1/2,1/2,E_+\rangle_{\psi_3=0},\\ &\langle 3/2,3/2|H_{DD}^{23}|1/2,1/2,E_+\rangle_{\psi_3=0}=0\end{aligned} \tag{35}$$

The first two matrix elements are equal and opposite because of the antisymmetry of $|1/2,1/2,E_+\rangle$ under the interchange of spins 2 and 3, while the last matrix element vanishes because H_{DD}^{23} and $|3/2,3/2\rangle$ are symmetric under interchange of spins 2 and 3, while $|1/2,1/2,E_+\rangle$ is antisymmetric (this is similar to the case of the two spin system considered in Ref. [14]). Finally, the transition rate Eq. (18) involves products of correlation functions of these matrix elements. In the abbreviated notation $|a\rangle=|1/2,1/2,E_+\rangle$ and $|b\rangle=|3/2,3/2\rangle$, the non-vanishing part of the integrand in Eq. (20) is given by

$$\overline{\langle a|H_{DD}^{12}|b\rangle_t\langle b|H_{DD}^{12}|a\rangle_{t+\tau}+\langle a|H_{DD}^{13}|b\rangle_t\langle b|H_{DD}^{12}|a\rangle_{t+\tau}+\langle a|H_{DD}^{12}|b\rangle_t\langle b|H_{DD}^{13}|a\rangle_{t+\tau}+\langle a|H_{DD}^{13}|b\rangle_t\langle b|H_{DD}^{13}|a\rangle_{t+\tau}}. \tag{36}$$

Finally, using the symmetry relations in Eq. (35), we see that this quantity vanishes identically owing to a cancellation:

$$\overline{2\langle a|H_{DD}^{12}|b\rangle_t\langle b|H_{DD}^{12}|a\rangle_{t+\tau}-2\langle a|H_{DD}^{12}|b\rangle_t\langle b|H_{DD}^{12}|a\rangle_{t+\tau}}\equiv 0. \tag{37}$$

This observation is in agreement with previous studies of dipolar relaxation in linear symmetric molecules [21,22]

Asymmetric linear systems (i.e., those with λ different from 1) also possess long-lived states. Evaluating A, B, and C for general values of λ and $\theta=\pi$ yields

$$\begin{aligned}&[A(\lambda,\theta)+B(\lambda,\theta)\cos 2\psi_3+C(\lambda,\theta)\sin 2\psi_3]_{\theta=\pi}\\ &\quad=\frac{5}{48\lambda^6(1+\lambda)^6}(r(\lambda)+s(\lambda)\sin 2\psi_3+t(\lambda)\cos 2\psi_3),\end{aligned} \tag{38}$$

where r, s, and t are polynomials that can be obtained by making appropriate substitutions in the expressions in Appendix A.3. Solving for ψ_3 in terms of λ yields the curve displayed in Fig. 2. For $\lambda = 1$ we return to the case of the symmetric linear system described above, and the mixing angle tends to zero. As λ becomes significantly larger than 1, the mixing angle tends to $\pi/3$. Referring to the discussion at the end of Section 2.1, we see that in this large-λ limit, where spin 3 is distant from spins 1 and 2, the long-lived state tends toward a singlet state of spins 1 and 2 as one would expect.

Scalar couplings that yield a state with a vanishing dipolar relaxation rate can be computed using the results in Appendix A.2. For instance, at $\lambda = 2$, we see from Fig. 2 that the dipolar decay rate of the state $|1/2, 1/2, E_+\rangle$ vanishes when $\psi_3 \simeq 0.307\pi \simeq 0.965$ radians, while the decay rate of $|1/2, 1/2, E_-\rangle$ vanishes when $\psi_3 \simeq 0.965 - \pi/2$ (modulo π). The latter value of ψ_3 is obtained, for instance, when $J_{12} \simeq 2.64$ Hz, $J_{13} \simeq -0.44$ Hz, and $J_{23} \simeq 0.1$ Hz, or any positive multiple of these values. As explained in more detail in Appendix A.2, this is just one example of a two-parameter family of possible scalar couplings, all of which yield the appropriate value of ψ_3.

4.1.2. Triangular molecules

In general, for physically realistic geometries, non-linear three-spin systems do not possess exact DSR states. To show this, it is enough to consider the quantity D in Eq. (27). Fig. 3 displays a contour plot of log D for triangular molecules as a function of λ and θ over a range of values. Although D is quite small for large values of λ, it does not strictly vanish anywhere on the domain considered in Fig. 3, apart from the lines $\theta = 0, \pi$, which correspond to linear systems discussed above. In Fig. 4 we display the mixing angle that yields the slowest decay rate as a function of λ for several values of θ. As in the case of linear systems, the mixing angle tends to $\pi/3$ at large values of λ, indicating that the small values of D at large values of λ correspond to a relatively long-lived singlet state of spins 1 and 2 that couples weakly to spin 3, which is well-separated from spins 1 and 2 in this limit.

Some insights can be gained from studying the behavior of D at large values of λ. Expanding Eq. (27) in a power series valid for large values of λ shows that it falls off as the eight power of the distance between spins 1 and 3:

$$D(\lambda \gg 1) \sim \frac{f(\theta)}{\lambda^8} \sim \frac{f(\theta)}{r_{13}^8}, \tag{39}$$

where $f(\theta)$ is a function of θ that can be computed using the expressions in Appendix A.3. The falloff of D seen at large distances is more rapid than might be naively expected from the form of the intramolecular dipolar Hamiltonian. Indeed, the transition rates involve two powers of the Hamiltonian, each of which falls off as $1/r^3$. It might therefore be expected that the rates would scale as $1/r^6$. The more rapid scaling seen in Eq. (39) is a consequence of the fact that the singlet state of spins 1 and 2 does not have any long-range dipolar fields. Rather, the long-range field created by spins 1 and 2 is quadrupolar, and falls off as $1/r^5$. Combining this with the $1/r^3$ falloff of the third spin's dipolar field, we find the $1/r^8$ dependence in Eq. (39). Note that this dependence is only found for the optimal choice of mixing angle that yields a singlet state of spins 1 and 2. The quantity D has, by definition, already been optimized in this respect. For other non-optimal choices of the mixing angle, the falloff of the decay rate can be slower.

Although triangular systems do not possess states that are strictly immune to intramolecular dipolar relaxation, systems that possess the optimal mixing angles displayed in Fig. 4 are still quite long-lived. To illustrate this, in Fig. 5 we display the enhancement factor E from Eq. (29), evaluated at the optimal value of the mixing angle ψ_3 for a range of λ and θ values. For moderate values of λ, sizable suppressions of the intramolecular dipolar decay rate are seen in the low-field system.

As a final example of a three-spin system, we consider the equilateral triangle ($\lambda = 1$ and $\theta = \pi/3$). This geometry occurs, for instance, in methyl groups. Evaluating A, B, and C yields $B = C = 0$, and hence

$$[A(\lambda,\theta) + B(\lambda,\theta)\cos 2\psi_3 + C(\lambda,\theta)\sin 2\psi_3]_{\lambda=1,\theta=\pi/3} = \frac{45}{64}. \tag{40}$$

In this case, the high degree of symmetry between the three spins yields an expression that is independent of ψ_3. However, in spite of this enhanced symmetry we conclude from Eq. (40) that the equilateral triangle does not possess any exact DSR states.

As noted in the introduction, previous work [23] on the three-spin equilateral triangle has indicated that this system possesses a state with vanishing intramolecular dipolar relaxation in the case of strongly anisotropic tumbling. We can see this explicitly by replacing the correlator in Eq. (21), which assumes isotropic tumbling, with the appropriate value for anisotropic tumbling. We have [23]

$$\begin{aligned}
&\int_{-\infty}^{+\infty} \overline{Y_{2M}(\hat{r}_{ij}(t))Y_{2M'}(\hat{r}_{kl}(t+\tau))}\mathrm{e}^{-\mathrm{i}\omega\tau}\mathrm{d}\tau \\
&\quad = \frac{3\delta_{M,-M'}}{8\pi} \\
&\qquad \times (-1)^M\left\{\frac{6D_1}{(6D_1)^2+\omega^2} + \frac{6D_1+12D_3}{(2D_1+4D_3)^2+\omega^2}\cos 2(\phi_{ij}-\phi_{kl})\right\} \\
&\quad \equiv \frac{3\delta_{M,-M'}}{8\pi}(-1)^M\{\xi_1(D_1,\omega) + \xi_2(D_1,D_3,\omega)\cos 2(\phi_{ij}-\phi_{kl})\},
\end{aligned} \tag{41}$$

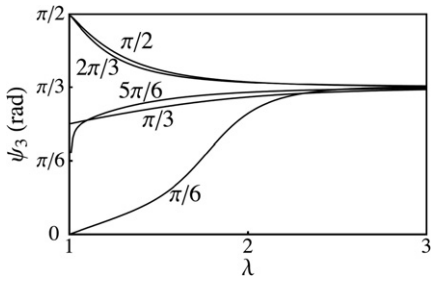

Fig. 4. Optimal mixing angle that minimizes the dipolar decay rate of the DSR states in triangular three-spin systems as a function of λ, for several values of θ.

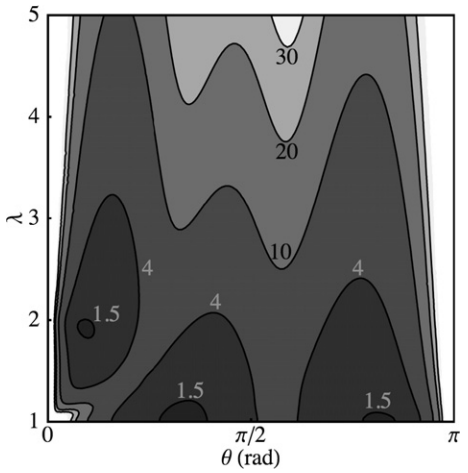

Fig. 5. Enhancement factor of Eq. (29) as a function of λ and θ in the three-spin system. The distance r_{12} has been scaled to 1. Note that the enhancement factor tends to infinity along the vertical lines $\theta = 0$ and $\theta = \pi$, corresponding to linear geometries.

where D_3 is the rotational diffusion coefficient for rotations about the axis of symmetry, D_1 is the coefficient for rotations about the orthogonal axes, and ϕ_{ij} and ϕ_{kl} are the azumithal spherical coordinates of the body-frame vectors $\hat{r}_{ij}$ and $\hat{r}_{kl}$, which for this particular geometry are taken to lie in the $x-y$ plane. We have normalized the correlator in Eq. (41) such that when $D_1 = D_3$ it reduces to the expression in Eq. (21) with $D_1 = D_3 = 1/\tau_c$. Re-evaluating the rate matrix from Eq. (31) using the correlator in Eq. (41) for the case of the equilateral triangle gives two contributions, proportional to ξ_1 and ξ_2, respectively:

$$W = \frac{3\mu_0^2\gamma^4\hbar^2}{40\pi^2 r_{12}^6}\frac{9}{16}\xi_1\left(\begin{array}{cccc|cc|cc} 1&2&2&0&0&0&0&0\\ 2&1&0&2&0&0&0&0\\ 2&0&1&2&0&0&0&0\\ 0&2&2&1&0&0&0&0\\ \hline 0&0&0&0&0&0&0&0\\ 0&0&0&0&0&0&0&0\\ \hline 0&0&0&0&0&0&0&0\\ 0&0&0&0&0&0&0&0 \end{array}\right) + \frac{3\mu_0^2\gamma^4\hbar^2}{40\pi^2 r_{12}^6}\frac{9}{64}\xi_2\left(\begin{array}{cccc|cc|cc} 0&0&0&0&1&4&1&4\\ 0&0&0&0&2&3&2&3\\ 0&0&0&0&3&2&3&2\\ 0&0&0&0&4&1&4&1\\ \hline 1&2&3&4&0&0&0&0\\ 4&3&2&1&0&0&0&0\\ \hline 1&2&3&4&0&0&0&0\\ 4&3&2&1&0&0&0&0 \end{array}\right) \tag{42}$$

As a check, in the limit $D_1 = D_3 = 1/\tau_c$ we regain the expression given in Eq. (31) after substituting $\lambda = 1$ and $\theta = \pi/3$. As in the case of isotropic tumbling, the rate matrix is independent of the mixing angle ψ_3. The long lifetime alluded to in [23] is found in the extreme narrowing limit ($\omega \ll D_{1,3}$) with $D_3 \gg D_1$. In this case, ξ_1 is much larger than ξ_2 and relaxation via the first term in Eq. (42) dominates. Hence the $j = 1/2$ states, which have decay rates proportional to ξ_2, are longer-lived than the $j = 3/2$ states, whose decay rates are proportional to ξ_1. However it may be inaccurate to describe such states as 'long-lived' in the present context. Indeed, in realistic situations the limit $D_3 \gg D_1$ occurs when D_1 is small because of a mechanical constraint on the molecular motion. This mechanical constraint leads to rapid relaxation because it implies a long correlation time for motion about the hindered axis, which in the extreme narrowing limit leads to rapid transition rates. Hence the limit $D_3 \gg D_1$ considered in [23] does imply that the $j = 1/2$ states are *longer*-lived than the $j = 3/2$ states; however the $j = 3/2$ states are quite short-lived, and the $j = 1/2$ states relax via the second term in Eq. (42) at a rate that need not be especially slow.

4.2. Four-spin system

Four-spin systems can be analyzed in a manner analogous to three-spin systems. The principal difference is that the geometry of the four-spin system cannot be specified as compactly. In general, three additional parameters are needed to specify the location of the fourth spin. We will therefore consider a few special cases that either possess long-lived states or that occur frequently in realistic molecules.

In block notation, the general form of the rate matrix Eq. (22) for the four-spin system is

$$W = \left[\begin{array}{c|c|c} W_{j=2\to j=2} & W_{j=2\to j=1} & W_{j=2\to j=0} \\ \hline W_{j=1\to j=2} & W_{j=1\to j=1} & 0 \\ \hline W_{j=0\to j=2} & 0 & 0 \end{array}\right], \tag{43}$$

where the blocks, from left-to-right or top-to-bottom, correspond to the $j = 2, j = 1$, and $j = 0$ states. The zeros in the lower right corner are a consequence of the selection rule Eq. (23). As described above, one consequence of these zeros is that the $j = 0$ populations can only equilibrate with the other levels via transitions to the $j = 2$ states (Fig. 1). For purposes of studying these transitions, the relevant submatrix is the 5-by-2 block $W_{j=0\to j=2}$, which has the simple form

$$W_{j=0\to j=2} = \begin{bmatrix} g & g & g & g & g \\ h & h & h & h & h \end{bmatrix}, \tag{44}$$

where g describes the rate of transitions to and from the level $|0,0,E_+\rangle$ and h describes the rate of transitions to and from the level $|0,0,E_-\rangle$. As in the three-spin case, g and h are functions of the spin system geometry and the mixing angle ψ_4. In addition, g and h differ only by the substitution $\psi_4 \to \psi_4 + \pi/2$. The general expressions for g and h are too lengthy to be included here, but certain special cases will be given below.

We now consider several particular geometries.

4.2.1. Linear systems

As in the three-spin system, linear spin systems containing four spins possess states whose dipolar decay rates vanish exactly. To illustrate this, we consider the linear symmetric geometry illustrated in Fig. 6. The two central spins are separated by unit distance, while the two outer spins are located a distance λ away from the central spins on either side. Evaluating the rates in Eq. (22) for the spin-zero states and casting the result in the form of Eq. (25), we obtain the functions A, B and C in terms of the geometrical parameter λ. The resulting expressions are given in Appendix A.4. Proceeding as in the analysis of Eq. (25), we minimize the decay rate with respect to the mixing angle, and find the values of ψ_4 for which the decay rate of the state $|0,0,E_+\rangle$ vanishes. Fig. 6 displays the resulting values of ψ_4. As $\lambda \to \infty$, $\psi_4 \to 0$, in which case the inner two spins (spins 1 and 2 in Fig. 6) form a singlet state that decouples from the outer two spins (spins 3 and 4), which are also in a singlet state.

4.2.2. Rectangular systems

The geometry of a rectangular system is shown in Fig. 7; the width of the system is scaled to unity, while the height is equal to λ. Without loss of generality, we assume $\lambda \geqslant 1$. As in the case of triangular molecules, we find that systems of this type do not in general possess exact DSR states for realistic geometries. At large values of λ they do, however, possess states with very slow intra-

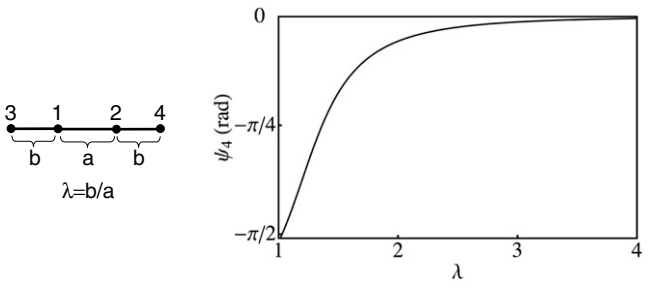

Fig. 6. Geometry of symmetric linear four-spin system (left) and mixing angle that yields an exact DSR state as a function of λ (right).

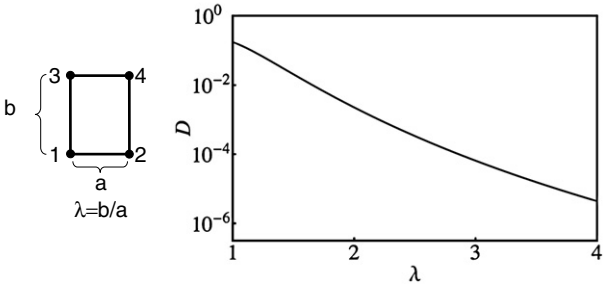

Fig. 7. Geometry of rectangular four-spin system (left) and discriminant function D from Eq. (27), on a semi-logarithmic scale, as a function of λ, with the distance a scaled to 1. Smaller values of D correspond to longer lifetimes.

molecular dipolar decay rates. Indeed, computing the rates from Eq. (22) and evaluating the quantity D from Eq. (27) gives the result illustrated in Fig. 7. This quantity, and hence the lower bound L, Eq. (26), on the intramolecular dipolar decay rate of the spin-zero states, is non-zero over the entire range of λ values in Fig. 7. In Fig. 8 we display the mixing angle that gives the slowest transition rate as a function of λ, for the $|0,0,E_+\rangle$ state.

In the limit of large λ, spins 1 and 2 are well separated from spins 3 and 4, and the mixing angle that minimizes the decay rate of the $|0,0,E_+\rangle$ state tends to zero. Referring to the basis set in Eq. (16), we see that the corresponding long-lived state consists of a state in which spins 1 and 2 are in a relative singlet, as are spins 3 and 4. The complete state is therefore a pair of well-separated, weakly interacting singlets. The leading behavior of D in this limit is

$$D(\lambda \gg 1) \sim \frac{1}{\lambda^{10}} \sim \frac{1}{r_{13}^{10}}. \tag{45}$$

The rapid falloff of the decay rate is accounted for by the fact that the two singlets interact via quadrupolar long-range fields. Since these fields fall off as $1/r^5$, the rate falls of as $1/r^{10}$.

Although rectangular systems do not possess exact DSR states, in some cases these systems do possess population imbalances in the spin-one levels that are immune to intramolecular dipolar relaxation because of a discrete symmetry. A full discussion of these symmetries is beyond the scope of this paper. However, one example of such a symmetry can be formulated in terms of the exchange operators P_{ab} that exchange the spin states of nuclei a and b. Referring to Fig. 7, we see that the combination $P_{12}P_{34}$ exchanges the spin states on opposite sides of the rectangle, while $P_{13}P_{24}$ exchanges the spin states on the top and bottom of the rectangle. Explicit computation shows that the intramolecular dipolar Hamiltonian is invariant under the action of the operator $P \equiv (P_{12}P_{34})(P_{13}P_{24})$. Referring to the basis states in Eqs. (10)–(13), we see that all of these states are eigenstates of P with eigenvalue +1 *except* for the states $|1,m\rangle_A$ and $|1,m\rangle_B$, which have eigenvalue -1. Just as in the case of the two-spin system, the states with eigenvalue -1 cannot equilibrate with states having eigenvalue +1 via intramolecular dipolar interactions. This gives rise to long-lived population imbalances between the states $|1,m\rangle_A$ and $|1,m\rangle_B$ and the remaining states. Of course, these long-lived populations *only* exist in systems having a high degree of spatial symmetry, and where the eigenstates of P are also eigenstates of the Hamiltonian. Certain specific combinations of scalar couplings are required in order to satisfy this condition. These long-lived population imbalances differ from DSR states because they involve two *families* of states that cannot equilibrate via intramolecular dipolar interactions. By contrast, exact DSR states are single states that cannot equilibrate with any other state.

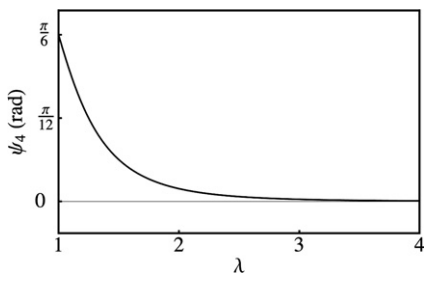

Fig. 8. Optimal mixing angle as a function of λ for the rectangular spin system.

In Fig. 9 we display the smallest eigenvalue of the matrix $W_{ab}^{\mathrm{High}} - \delta_{ab}\sum_c W_{ac}^{\mathrm{High}}$ appearing in Eq. (29) divided by each of the 15 non-trivial eigenvalues of $W_{ab}^{\mathrm{Low}} - \delta_{ab}\sum_c W_{ac}^{\mathrm{Low}}$. This yields a total of 15 non-trivial ratios, each of which measures the lifetime enhancement of a particular relaxation mode of the low-field system. These ratios are plotted on a semi-logarithmic scale as a function of ψ_4 for two representative values of the Euler angles (α,β,γ) (see Eq. (17)) and with $\lambda = 3/2$. In the absence of an exact DSR state, the analysis of these plots is complicated by the fact that the decay modes generally involve admixtures of populations in many states. However we can still make some qualitative comments. In both panels, we see that two of the eigenvalue ratios, labeled by C_1 and C_2, show a strong dependence on the mixing angle ψ_4. These decay modes have sizable populations in one of the spin-zero states. The approximate DSR mode corresponds to the higher of the two curves, namely C_2. The choice of Euler angles in the left panel of Fig. 9 results in relatively long-lived spin-1 decay modes, as described in the preceding paragraph, while the values on the right are further from the highly symmetric values that yield long lifetimes. These long-lived spin-1 decay modes are indicated by the (nearly flat) curves labeled C_3. In both panels, the approximate DSR modes are among the longest-lived modes of the low-field system, possessing enhancement factors that range from roughly 5–10 depending upon the Euler angles. Larger enhancement factors (~50) are seen for the spin-1 modes, particularly for small values of the Euler angles such as those shown in the left panel of Fig. 9.

4.2.3. A planar non-linear system with long-lived states

Although the rectangular system does not possess an exact DSR state, a variety of other non-collinear geometries can be found that do possess such states. In Fig. 10 we display a sample planar geometry where spins 1 and 2 are separated by unit distance along the y axis, and spins 3 and 4 are located at positions x_3 and x_4 along the x axis. The functions A, B, and C are given in Appendix A.6. Owing to the high degree of symmetry between spins 1 and 2, in this case we find that a cancellation similar to that illustrated above in Eqs. (34)–(37) leads to $C = 0$. This implies that the decay rates have the simplified form

$$\sum_{\mathrm{X}} W_{|0,0,E_+\rangle\to|\mathrm{X}\rangle} = \frac{3\mu_0^2\gamma^4\hbar^2\tau_c}{40\pi^2 r_{12}^6}[A(x_3,x_4) + B(x_3,x_4)\cos 2\psi_4]. \tag{46}$$

Because the rates must always be positive, we conclude that $A(x_3,x_4) \geqslant |B(x_3,x_4)|$, for if this were not the case the rate could be negative for certain values of the mixing angle. We have verified this inequality numerically for $-10 < x_3, x_4 < 10$. We conclude that the dipolar decay rate vanishes only when $A(x_3,x_4) = |B(x_3,x_4)|$ and $\psi_4 = 0$ (in the case $B(x_3,x_4) < 0$) or $\pi/2$ (in the case $B(x_3,x_4) > 0$).

In Fig. 10 we display D as a function of x_3 and x_4. We see that D vanishes along the line $x_3 = x_4$ as well as for values of x_3 and x_4 lying along the curve labeled C_1. For these particular configurations, the system possesses an exact DSR state for suitable values of the mixing angle ψ_4. Inspecting the values of A and B along the line $x_3 = x_4$ and the curve C_1 we find that both sets of exact DSR

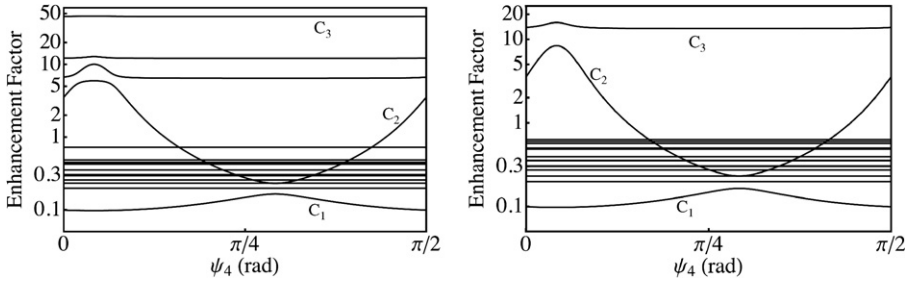

Fig. 9. Enhancement factors for all decay modes of the four-spin system as a function of the mixing angle ψ_4 for $\lambda = 3/2$ and two values of the spin-1 Euler angles. Left: $\alpha = 0$, $\beta = 0$, $\gamma = \pi/10$. Right: $\alpha = \pi/4$, $\beta = \pi/3$, $\gamma = -\pi/3$.

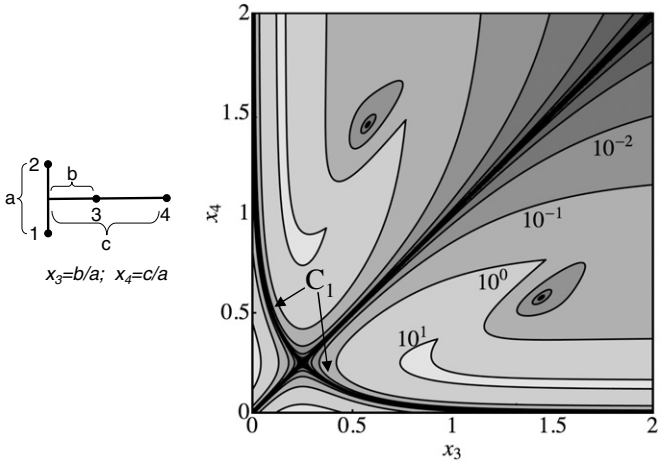

Fig. 10. Left: Geometry of planar four-spin system. Right: Discriminant function D as a function of x_3 and x_4. On the right, the distance a has been scaled to 1. Smaller values of D correspond to longer lifetimes.

states have $\psi_4 = 0$, corresponding to a state where spins 1 and 2 are in a relative singlet, as are spins 3 and 4. The exact DSR states along the line $x_3 = x_4$ therefore correspond to a degenerate, unphysical case where spins 3 and 4 coalesce into a point-like singlet, while spins 1 and 2 form a second singlet. The exact DSR states along the curve C_1 correspond to a combined state of a 'vertical' singlet formed by spins 1 and 2, and a second 'horizontal' singlet formed by spins 3 and 4 (in the orientation of Fig. 10). These two singlets are situated such that neither singlet interferes with the singlet order of the other. In the limit where spin 4 is very distant from the other spins (i.e., $x_4 \to \infty$) we see that the configuration with an exact DSR state corresponds to a linear arrangement of spins 1,2 and 3 (i.e. $x_3 \to 0$), with spins 1 and 2 in a singlet. After a trivial re-labeling of the spins, this corresponds well with the exact DSR state of the linear three-spin system that was discussed above.

It is tempting to speculate that the exact DSR states along the curve C_1, comprised of two orthogonal singlet pairs, may have some simple geometrical property that accounts for the absence of inter-singlet relaxation. However, this appears not to be the case. The absence of intramolecular dipolar relaxation in these states is the result of an interference effect that can be understood as follows. First, because these states are antisymmetric under interchange of either spins 1 and 2 or spins 3 and 4, the dipolar interactions between spins 1 and 2 vanish, as do those between spins 3 and 4. The only non-vanishing dipolar matrix elements correspond to interactions between a spin in the first singlet (i.e., spins 1 and 2) and a spin in the second singlet (i.e., spins 3 and 4). Second, owing to the geometrical symmetry between spins 1 and 2, the spatial correlation functions appearing in Eq. (20) take a simple form. The decay rate of states with $\psi_4 = 0$ can therefore be written as

$$\sum_X W_{|0,0,E_+\rangle_{\psi_4=0} \to |X\rangle} \propto \frac{1}{r_{13}^6}[1 - P_2(\cos\theta_{12,23})] + \frac{1}{r_{14}^6}[1 - P_2(\cos\theta_{14,24})] - \frac{2}{r_{13}^3 r_{14}^3}[P_2(\cos\theta_{13,14}) - P_2(\cos\theta_{13,24})]. \quad (47)$$

The first term in square brackets is non-negative, and results from dipolar interactions with spin 3. The second term is also non-negative, and results from dipolar interactions with spin 4. The last term, however, can be positive or negative, and results from interference between interactions with spin 3 and spin 4. For the exact DSR configurations described in the previous paragraph, the last term cancels the first two. Indeed, re-expressing Eq. (46) in terms of the variables x_3 and x_4, with $x_4 \geqslant x_3$, we find

$$\sum_X W_{|0,0,E_+\rangle_{\psi_4=0} \to |X\rangle} \propto \left(\frac{x_3}{(1+4x_3^2)^{5/2}} - \frac{x_4}{(1+4x_4^2)^{5/2}} \right)^2. \quad (48)$$

This quantity vanishes when $x_3 = x_4$ and for values of x_3 and x_4 that satisfy

$$\frac{x_3}{(1+4x_3^2)^{5/2}} = \frac{x_4}{(1+4x_4^2)^{5/2}}. \quad (49)$$

It is these latter solutions that correspond to the points along curve C_1.

Referring to Fig. 10, we see that the planar system possesses four more exact DSR states located at the points $(x_3, x_4) \approx \pm(0.5757, 1.4423)$, as well as the symmetric points obtained by interchanging spins 3 and 4. At each of these points, we find that B is positive, implying that the mixing angle ψ_4 for these states is equal to $\pi/2$ (see Eq. (46)). In contrast to the states considered in the previous paragraph, these states do not correspond to a combination of singlet states. Indeed, referring to the discussion at the end of Section 2.2, we see that this value of ψ_4 does not correspond to any pairwise combination of singlets in the state $|0, 0, E_+\rangle$.

4.2.4. A sample non-planar system with long-lived states

In Fig. 11 we display a sample non-planar geometry for the four-spin system. The system is obtained by modifying the rectangular geometry of Fig. 7 by rotating one pair of spins out of the plane of the molecule by an angle ϕ. Without loss of generality, we assume that $0 \leqslant \phi \leqslant \pi/2$, because geometries with values of ϕ outside this range are related to those within this range by a simple relabelling of the spins. For special choices of the geometrical parameters λ and ϕ, the system reduces to a rectangle or tetrahedron. The expressions for the functions A, B and C are given in Appendix A.7 for the case $\phi = \pi/2$; the expressions for general values of ϕ are too lengthy to be included in full. As in the previous examples, we compute the quantity D from Eq. (27) as a function of λ and ϕ. Fig. 11 shows a contour plot of D as a function of λ and ϕ. The system possesses states with vanishing dipolar relaxa-

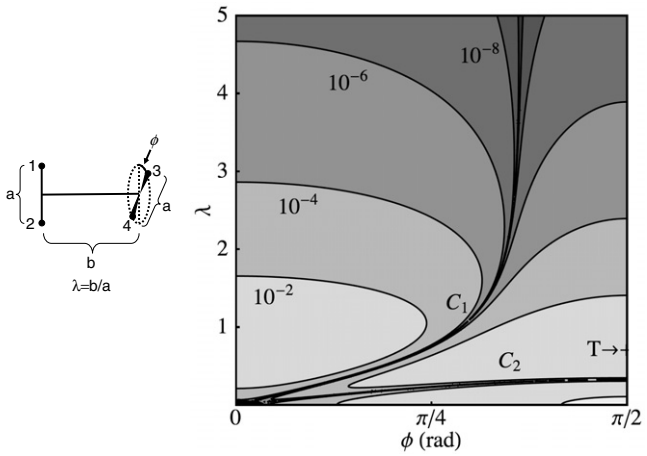

Fig. 11. Left: Geometry of non-planar four-spin system. Note that spins 3 and 4 are rotated *out of plane* by an angle ϕ, while the line connecting spins 3 and 4 is kept perpendicular to the central horizontal line of length b. When $\phi = 0$ the system reduces to a rectangular geometry. Right: Discriminant function D as a function of λ and ϕ. The tickmark labeled 'T' on the right-hand border indicates values of λ and ϕ that yield a tetrahedral geometry. In the figure on the right, the distance a has been scaled to 1. Smaller values of D correspond to longer lifetimes.

tion rates along two curves in the parameter space, which we label as C_1 and C_2. In Fig. 12 we display the values of ψ_4 that yield long-lived states along these two curves. Note that, along both of the curves C_1 and C_2, for values of λ approaching zero, the systems with exact DSR states have values of ϕ that also tend to zero. Referring to Fig. 11, we see that, in this limit, spins 1 and 3 approach one another, as do spins 2 and 4. Furthermore, from Fig. 12, we see that for small values of λ the mixing angle ψ_4 approaches $\pi/3$. Referring to the discussion at the end of Section 2.2, this corresponds to a singlet state of spins 1 and 3, together with a separate singlet state of spins 2 and 4. Hence, the system tends towards a pair of nearly point-like singlets that are well separated (in comparison to their size) as λ approaches zero, as one would expect. Likewise, as λ tends to larger values along the curve C_1, the mixing angle tends to zero. In this limit, spins 1 and 2 are well-separated from spins 3 and 4, and the exact DSR state tends toward a singlet state of spins 1 and 2 together with a second singlet state of spins 3 and 4.

A tetrahedral geometry is obtained by setting $\lambda = 1/\sqrt{2}$ and $\phi = \pi/2$. The corresponding point is indicated by a tickmark labeled 'T' on the right-hand border of Fig. 11. We conclude that tetrahedral molecules do not possess exact DSR states; indeed, the lifetime of the tetrahedral system, as measured by the quantity D, is relatively short in comparison to neighboring geometries. However, as in the case of the equilateral triangle, this highly symmetric geometry leads to transition rates from the two spin-zero states that are equal and that do not depend on ψ_4. In terms of the functions g and h, we have $g = h = 3/16$ (see Eq. (44)). Moreover, computation of the full

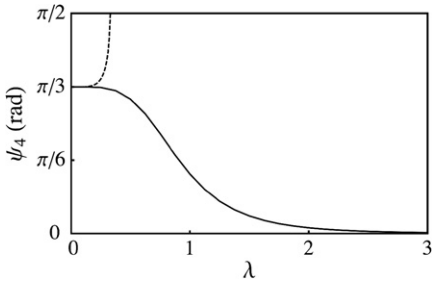

Fig. 12. Mixing angles that yield exact DSR states in non-planar four-spin system as a function of λ. Solid curve corresponds to curve C_1 in Fig. 11; dashed curve corresponds to C_2. The dashed curve terminates at $\lambda \sim 1/3$ because this is the largest value of λ attained along the curve C_2.

decay matrix, including the $j = 1$ states, shows that the tetrahedral system does not possess long-lived population imbalances of the sort found above in the rectangular system.

4.3. Larger numbers of spins

The above analysis can be extended to systems containing more than four spins. Indeed, one might expect the lowest-spin states of arbitrary systems to possess relaxation bottlenecks of the sort described here. However, the $N > 4$ cases differ from the cases $N = 2, 3, 4$ in that the number of states possessing the lowest possible total spin (namely $j = 0$ for N even and $j = 1/2$ for N odd) is significantly larger. Indeed, the five-spin system has ten states (five doublets) with $j = 1/2$, while the six-spin system has five $j = 0$ states. As a result, compact expressions for the lowest-spin energy eigenstates, such as in Eqs. (8) and (16), are not generally possible. The low-spin eigenstates depend on a larger number of mixing angles, which in turn complicates the analysis of their lifetimes.

A second difference between the cases $N = 2, 3, 4$ and the case of N odd and larger than three is that, in the latter case, the $j = 1/2$ states can undergo direct transitions to both the $j = 3/2$ and $j = 5/2$ states. Consequently, in order to have a long-lived DSR state, these systems must be arranged in such a way that *both* of these relaxation pathways are suppressed. Systems with N even and larger than four are similar to the $N = 4$ system because the spin-zero populations in these systems can only equilibrate via transitions to the $j = 2$ states. Transitions to the $j = 1$ levels, and to the levels with $j > 2$, are forbidden by the selection rule in Eq. (23).

Yet another difference between the cases $N = 2, 3, 4$ and cases with larger N is that, in the latter case, the transition rates depend on two sets of mixing angles, namely the mixing angles of the lowest-spin states *and* the mixing angles of the higher spin states. In the cases $N = 2, 3, 4$, the states that are accessible from the lowest-spin states also happen to have the maximum total spin. As a consequence, these states are independent of the scalar couplings, as seen in Eqs. (2) and (10), and do not involve any mixing angles. By contrast, in the six-spin system, for example, the spin-zero states can make transitions to any one of five spin-two multiplets. These five multiplets will depend on a family of mixing angles that depend, in turn, on the scalar couplings.

Though these considerations do not show that long-lived states do not exist in systems with more than four strongly coupled spins, they do illustrate the complications encountered in these systems.

In systems with more than four spins that contain a subset of two, three or four isolated spins that couple weakly to the remaining spins, the isolated subset can possess long-lived states of the sort described in the preceding sections. The lifetimes of these states will be shortened by couplings between the isolated subset and the remaining spins; the degree of shortening can be estimated using standard perturbative techniques.

5. Conclusion

The examples described in the preceding sections show that a wide variety of spin systems can possess states that are immune to intramolecular dipolar relaxation in the extreme narrowing limit. Even in systems that do not possess 'dipole selection rule' long-lived states whose dipolar decay rates vanish exactly (such as the rectangular four-spin system), discrete symmetries can result in long-lived population imbalances. The results presented above and in Appendices can be used to systematically search for systems that should possess long-lived states, and to determine what role, if any, the selection rule in Eq. (23) plays in the determining the relaxation times of these systems.

Appendix A

A.1. Eigenvalues and eigenvectors for four-spin case

The eigenvalues of $j = 0$ block of the four-spin Hamiltonian H given in Eq. (15) are

$$E_{\pm} = \frac{\pi}{2}[-\bar{J} \pm \Delta], \tag{A1.1}$$

where $\bar{J} = \sum_{k<l} J_{kl}$ and Δ is given by

$$\Delta = 2\sqrt{\bar{J}^2 - 3(J_{12}[J_{13}+J_{14}+J_{23}+J_{24}] + J_{13}[J_{14}+J_{23}+J_{34}] + J_{14}[J_{24}+J_{34}] + J_{23}[J_{24}+J_{34}] + J_{24}J_{34})}. \tag{A1.2}$$

The eigenvectors are given by Eq. (16), where the mixing angle ψ_4 is given by

$$\psi_4 = -\tan^{-1}\left(\frac{\sqrt{3}[J_{13}-J_{14}-J_{23}+J_{24}]}{J_{13}+J_{23}+J_{14}+J_{24}-2(J_{12}+J_{34})+\Delta}\right). \tag{A1.3}$$

A.2. Mixing angles

Here we show that it is mathematically possible to select scalar couplings that will yield any chosen value of the mixing angle ψ_N in the three- and four-spin systems. This task is essentially the inverse of the usual process of finding the eigenvectors (and hence the mixing angle) from the scalar couplings. For any given mixing angle ψ_N, *any* matrix of the form

$$Q(E_+, E_-, \psi_N) \equiv \begin{bmatrix} \cos\psi_N & -\sin\psi_N \\ \sin\psi_N & \cos\psi_N \end{bmatrix}\begin{bmatrix} E_+ & 0 \\ 0 & E_- \end{bmatrix}\begin{bmatrix} \cos\psi_N & \sin\psi_N \\ -\sin\psi_N & \cos\psi_N \end{bmatrix} = \begin{bmatrix} \cos^2\psi_N E_+ + \sin^2\psi_N E_- & (E_+ - E_-)\sin\psi_N\cos\psi_N \\ (E_+ - E_-)\sin\psi_N\cos\psi_N & \sin^2\psi_N E_+ + \cos^2\psi_N E_- \end{bmatrix} \tag{A2.1}$$

will, by construction, have eigenvalues E_+ and E_- with mixing angle ψ_N. Care has been taken to ensure that the sign conventions in Eq. (A2.1) match those in Eqs. (8) and (16). A set of scalar couplings that yield the desired mixing angle may be determined by (i) choosing two arbitrary energy eigenvalues E_+ and E_- satisfying $E_+ \geqslant E_-$ (the inequality is a consequence of Eqs. (7) and (A1.1)), (ii) computing the matrix Q, and (iii) solving the linear system of equations

$$H(J_{kl}) = Q(E_+, E_-, \psi_N) \tag{A2.2}$$

for the couplings J_{kl}. The Hamiltonians $H(J_{kl})$ for the three- and four-spin systems have been given in Eqs. (6) and (15). In the three-spin case, the system Eq. (A2.2) comprises three independent equations for the three couplings J_{12}, J_{13}, and J_{23}. The result is a family of scalar couplings parametrized in terms of the two energy eigenvalues E_+ and E_-. The four-spin case involves a total of six scalar couplings, and consequently the system of Eq. (A2.2) yields a family of solutions parametrized by two energy eigenvalues and three undetermined scalar couplings; any values of these undetermined couplings will yield a Hamiltonian with the chosen energy eigenvalues and mixing angle. In the three-spin system, the solution to the system of Eq. (A2.2) is

$$\begin{aligned} 2\pi J_{12} &= -\frac{1}{3}(2[E_- + E_+] + [E_- - E_+][\cos 2\psi_3 - \sqrt{3}\sin 2\psi_3]) \\ 2\pi J_{13} &= -\frac{1}{3}(2[E_- + E_+] + [E_- - E_+][\cos 2\psi_3 + \sqrt{3}\sin 2\psi_3]) \\ 2\pi J_{23} &= -\frac{4}{3}(E_+\cos^2\psi_3 + E_-\sin^2\psi_3). \end{aligned} \tag{A2.3}$$

In the four-spin system, the solution to the system of Eq. (A2.2) is

$$\begin{aligned} 2\pi J_{12} &= -\frac{1}{3}(3(2\pi J_{34}) + 4E_+\cos^2\psi_4 + 4E_-\sin^2\psi_4) \\ 2\pi J_{13} &= -\frac{1}{3}(2[E_- + E_+] + 3(2\pi J_{24}) + [E_- - E_+][\cos 2\psi_4 - \sqrt{3}\sin 2\psi_4]) \\ 2\pi J_{14} &= -\frac{1}{3}(2[E_- + E_+] + 3(2\pi J_{23}) + [E_- - E_+][\cos 2\psi_4 + \sqrt{3}\sin 2\psi_4]). \end{aligned} \tag{A2.4}$$

A.3. A, B and C for the three-spin system

For the three-spin system illustrated in Fig. 2, the functions A, B and C are given by

$$\begin{aligned} A(\lambda,\theta) &= \frac{5}{96}\left\{4 + \frac{4}{Q^3} - \frac{4}{Q^{5/2}} - \frac{\lambda^3 + 4\lambda^5 + \lambda^8 + Q^{5/2}[\lambda^3 - 4]}{Q^{5/2}\lambda^6} + \frac{8\lambda[\lambda^3+1]\cos\theta - 3[1 + Q^{5/2} + \lambda^5]\cos 2\theta}{Q^{5/2}\lambda^3}\right\} \\ B(\lambda,\theta) &= \frac{5}{96Q^3\lambda^6}\left\{2Q^3[1 - \lambda^3 + \lambda^6] - 4\lambda^6 + Q^{1/2}\lambda^3[1 + 4\lambda^2 + 4\lambda^3 + \lambda^5 - 8\lambda(1+\lambda^3)\right. \\ &\quad \left.\times\cos\theta + 3(1 - 2Q^{5/2} + \lambda^5)\cos 2\theta]\right\} \\ C(\lambda,\theta) &= -\frac{5}{16\sqrt{3}}\left\{1 - \frac{1}{\lambda^6} + \frac{1 + 4\lambda^2 - 4\lambda^3 - \lambda^5 + 8\lambda[\lambda^3 - 1]\cos\theta - 3[\lambda^5 - 1]\cos 2\theta}{2Q^{5/2}\lambda^3}\right\}, \end{aligned} \tag{A3.1}$$

where $Q = 1 + \lambda^2 - 2\lambda\cos\theta$.

A.4. A, B, and C for the symmetric linear four-spin system

For the symmetric linear four-spin system illustrated in Fig. 4, the functions A, B and C are given by

$$\begin{aligned}
A(\lambda) &= \frac{5}{24\lambda^6}\left\{\frac{3[1+3\lambda(1+\lambda)]^2}{(1+\lambda)^6} + \frac{(1+9\lambda+33\lambda^2+62\lambda^3+60\lambda^4+12\lambda^5-48\lambda^6-66\lambda^7-36\lambda^8-8\lambda^9)^2}{(1+3\lambda+2\lambda^2)^6}\right\}\\
B(\lambda) &= -\frac{5}{24}\left\{1-\frac{2}{(1+\lambda)^6}-\frac{8}{(1+\lambda)^3}-\frac{12}{(1+\lambda)^2}+\frac{1}{(1+2\lambda)^6}+\frac{2}{(1+2\lambda)^3}+\frac{96}{(1+2\lambda)^2}-\frac{2+4\lambda^3[3\lambda-1]}{\lambda^6}\right\}\\
C(\lambda) &= -\frac{5}{4\sqrt{3}}\left\{\frac{1}{\lambda^6}-\frac{1}{(1+\lambda)^6}+\frac{1}{(1+\lambda)^3}+\frac{1}{(1+3\lambda+2\lambda^2)^3}-\frac{(1+2\lambda)^3+1}{\lambda^3(1+2\lambda)^3}\right\},
\end{aligned} \tag{A4.1}$$

A.5. A, B and C for the rectangular four-spin system

For the rectangular four-spin system of Fig. 7,

$$\begin{aligned}
A(\lambda) &= \frac{5}{12}\left\{2+\frac{1}{\lambda^3}+\frac{2}{\lambda^6}+\frac{1}{(1+\lambda^2)^3}\right.\\
&\quad\left.+\frac{1-2\lambda^2-2\lambda^3+\lambda^5}{\lambda^3(1+\lambda^2)^{5/2}}+\frac{1-4\lambda^2+\lambda^4}{(1+\lambda^2)^5}\right\}\\
B(\lambda) &= -\frac{5}{24}\left\{4+\frac{2}{\lambda^3}-\frac{2}{\lambda^6}-\frac{1}{(1+\lambda^2)^3}\right.\\
&\quad\left.-\frac{4-8\lambda^2+4\lambda^3-2\lambda^5}{\lambda^3(1+\lambda^2)^{5/2}}-\frac{1-4\lambda^2+\lambda^4}{(1+\lambda^2)^5}\right\}\\
C(\lambda) &= -\frac{5}{8\sqrt{3}}\left\{\frac{2}{\lambda^3}+\frac{2}{\lambda^6}-\frac{1}{(1+\lambda^2)^3}\right.\\
&\quad\left.+\frac{4-2\lambda^2}{(1+\lambda^2)^{5/2}}-\frac{1-4\lambda^2+\lambda^4}{(1+\lambda^2)^5}\right\}.
\end{aligned} \tag{A5.1}$$

A.6. A, B, and C for the planar four-spin system

For the planar four-spin system of Fig. 10,

$$\begin{aligned}
\frac{1}{5}A(x_3,x_4) &= \frac{1+\Delta^3+\Delta^6}{24\Delta^6}+\frac{16}{3}\left(\frac{1}{P_3^3}+\frac{1}{P_4^3}\right)\\
&\quad-\frac{8}{3}\left(\frac{1-16x_3^2+16x_3^4}{P_3^5}\right.\\
&\quad\left.+\frac{1-16x_4^2+16x_4^4}{P_4^5}\right)\\
&\quad-\frac{1}{3\Delta^3}\left(\frac{1-8x_3^2+2\Delta^3[1-2x_3^2]}{P_3^{5/2}}\right.\\
&\quad\left.+\frac{1-8x_4^2+2\Delta^3[1-2x_4^2]}{P_4^{5/2}}\right)\\
&\quad+\frac{16}{3}\left(\frac{1-36x_3x_4-2[x_3^2+x_4^2]+16x_3^2x_4^2}{P_3^{5/2}P_4^{5/2}}\right)\\
\frac{1}{5}B(x_3,x_4) &= -\frac{1+\Delta^3+\Delta^6}{24\Delta^6}+\frac{8}{3}\left(\frac{1}{P_3^3}+\frac{1}{P_4^3}\right)\\
&\quad-\frac{16}{3}\left(\frac{1-16x_3^2+16x_3^4}{P_3^5}+\frac{1-16x_4^2+16x_4^4}{P_4^5}\right)\\
&\quad+\frac{1}{3\Delta^3}\left(\frac{1-8x_3^2+2\Delta^3[1-2x_3^2]}{P_3^{5/2}}\right.\\
&\quad\left.+\frac{1-8x_4^2+2\Delta^3[1-2x_4^2]}{P_4^{5/2}}\right)\\
&\quad-\frac{16}{3}\left(\frac{1+36x_3x_4-2[x_3^2+x_4^2]+16x_3^2x_4^2}{P_3^{5/2}P_4^{5/2}}\right)
\end{aligned} \tag{A6.1}$$

Where $P_{3,4} = (1+4x_{3,4}^2)$, $\Delta = (x_3 - x_4)$, and we have taken $x_4 \geqslant x_3$.

A.7. A, B, and C for the three-dimensional four-spin system

The general expressions for A, B, and C for the system of Fig. 11 are too lengthy to report here. For the special case $\phi = 0$, the expressions reduce to those given for the rectangular system in Appendix A.5. For the case $\phi = \pi/2$,

$$\begin{aligned}
\frac{1}{5}A(\lambda,\phi=\pi/2) &= \frac{1}{24}+\frac{6}{(1+2\lambda^2)^5}-\frac{4}{(1+2\lambda^2)^4}\\
&\quad+\frac{4}{3(1+2\lambda^2)^3}-\frac{1}{\sqrt{2}(1+2\lambda^2)^{5/2}}\\
&\quad+\frac{\sqrt{2}}{3(1+2\lambda^2)^{3/2}}\\
\frac{1}{5}B(\lambda,\phi=\pi/2) &= -\frac{1}{5}A(\lambda,\phi=\pi/2)+\frac{6}{(1+2\lambda^2)^5}\\
C(\lambda,\phi=\pi/2) &= 0.
\end{aligned} \tag{A7.1}$$

References

[1] M. Carravetta, O.G. Johannesson, M.H. Levitt, Beyond the T1 limit: singlet nuclear spin states in low magnetic fields, Phys. Rev. Lett. 92 (2004) 153003.
[2] M. Carravetta, M.H. Levitt, Long-lived nuclear spin states in high-field solution NMR, J. Am. Chem. Soc. 126 (2004) 6228–6229.
[3] R. Sarkar, P.R. Vasos, G. Bodenhausen, Singlet-exchange NMR spectroscopy for the study of very slow dynamic processes, J. Am. Chem. Soc. 129 (2006) 328–334.
[4] K. Golman, O. Axelsson, H. Johannesson, S. Mansson, C. Olofsson, J.S. Petersson, Parahydrogen-induced polarization in imaging: subsecond 13C angiography, Magn. Reson. Med. 46 (2001) 1–5.
[5] K. Golman, J.H. Ardenkjaer-Larsen, J. Svensson, O. Axelsson, G. Hansson, L. Hansson, H. Johannesson, I. Leunbach, S. Mansson, J.S. Petersson, G. Petersson, R. Servin, L.G. Wistrand, C13 angiography, Acad. Radiol. 9 (2002) S506–S510.
[6] E. Johansson, L.E. Olsson, S. Mansson, J.S. Petersson, K. Golman, F. Stahlberg, R. Wirestam, Perfusion assessment with bolus differentiation: a technique applicable to hyperpolarized tracers, Magn. Reson. Med. 52 (2004) 1043–1051.
[7] E. Johansson, S. Mansson, R. Wirestam, J. Svensson, J.S. Petersson, K. Golman, F. Stahlberg, Cerebral perfusion assessment by bolus tracking using hyperpolarized 13C, Magn. Reson. Med. 51 (2004) 464–472.
[8] S. Kohler, Y. Yen, J. Wolber, A.P. Chen, M.J. Albers, R. Bok, V. Zhang, J. Tropp, S. Nelson, D. Vigneron, J. Kurhanewicz, R.E. Hurd, In vivo C13 metabolic imaging at 3T with hyperpolarized C13-1-pyruvate, Magn. Reson. Med. 58 (2007) 65–69.
[9] K. Golman, R. 't Zandt, M. Thaning, Real-time metabolic imaging, Proc. Natl. Acad. Sci. USA 103 (2006) 11270–11275.
[10] K. Golman, J.S. Petersson, Metabolic imaging and other applications of hyperpolarized C13, Acad. Radiol. 13 (2006) 932–942.
[11] K. Gopalakrishnan, G. Bodenhausen, Lifetimes of the singlet-states under coherent off-resonance irradiation in NMR spectroscopy, J. Magn. Reson. 182 (2006) 254–259.
[12] R. Sarkar, A. Puneet, D. Moskau, P.R. Vasos, G. Bodenhausen, Extending the scope of singlet-state spectroscopy, ChemPhysChem 8 (2007) 2652–2656.
[13] S. Cavadini, P.R. Vasos, Singlet states open the way to longer time-scales in the measurement of diffusion by NMR spectroscopy, Concepts Magn. Reson. A 32 (2007) 68–78.
[14] M.H. Levitt, M. Carravetta, Theory of long-lived spin states in solution nuclear magnetic resonance. I. Singlet states in low magnetic fields, J. Chem. Phys. 122 (2005) 214505–214514.

[15] G. Pileio, M. Concistre, M. Carravetta, M.H. Levitt, Long-lived nuclear spin states in the solution NMR of four-spin systems, J. Magn. Reson. 182 (2006) 353–357.
[16] C. Aroulanda, L. Storovoytova, D. Canet, Longitudinal nuclear spin relaxation of ortho- and para-hydrogen dissolved in organic solvents, J. Phys. Chem. A 111 (2007) 10615–10624.
[17] T. Jonischkeit, U. Bommerich, J. Stadler, K. Woelk, H.G. Niessen, J. Bargon, Generating long-lasting H-1 and C-13 hyperpolarization in small molecules with parahydrogen-induced polarization, J. Chem. Phys. 124 (2006).
[18] G. Pileio, M.H. Levitt, *J*-Stabilization of singlet states in the solution NMR of multiple-spin systems, J. Magn. Reson. 187 (2007) 141–145.
[19] E. Vinogradov, A.K. Grant, Long-lived states in solution NMR: selection rules for intramolecular dipolar relaxation in low magnetic fields, J. Magn. Reson. 188 (2007) 176–182.
[20] A. Abragam, The Principles of Nuclear Magnetism, Clarendon Press, Oxford, 1961.
[21] R.L. Vold, R.R. Vold, Nuclear magnetic relaxation in coupled spin systems, Prog. Nucl. Mag. Res. Sp. 12 (1977) 79–133.
[22] A.D. Bain, R.M. Lynden-Bell, Relaxation matrices for AX2 and AX3 nuclear spin systems, Mol. Phys. 30 (1975) 325–356.
[23] P.S. Hubbard, Nonexponential relaxation of three-spin systems in nonspherical molecules, J. Chem. Phys. 51 (1969) 1647–1651.